

Output characteristics of a 2.05 μm narrow-linewidth small-signal thulium-doped fiber amplifier under different pumping schemes

Xiaolong Sun(孙小龙), Zhijian Huang(黄智健), Miaomiao Yang(杨苗苗), Menghua Jiang(姜梦华), Tingwu Ge(葛廷武), Wenbin Qin(秦文斌), Youqiang Liu(刘友强), Yinhua Cao(曹银花), Zhiyong Wang(王智勇)

Citation: Chin. Phys. B. 35, 094212 (2026). DOI: 10.1088/1674-1056/ae4461 |
CSTR: 32038.14.CPB.ae4461
http://cpb.iphy.ac.cn; http://iopscience.iop.org/cpb

What follows is a list of articles you may be interested in

Dissipative soliton operation in a mode-locked laser based on thulium-doped fiber

Wen-Yan Zhang(张文艳), Lei Zheng(郑磊), Tian Zhang(张添), Nan-Nan Liu(刘楠楠), Li-Jie Geng(耿利杰), Kun Yang(杨坤), Li Zhan(詹黎)

Chin. Phys. B. 35, 044201 (2026). DOI: 10.1088/1674-1056/ae063c | CSTR: 32038.14.CPB.ae063c

Sequential generation of self-starting diverse operations in all-fiber laser based on thulium-doped fiber saturable absorber

Pei Zhang(张沛), Kaharudin Dimyati, Bilal Nizamani, Mustafa M. Najm, S. W. Harun

Chin. Phys. B. 31, 064204 (2022). DOI: 10.1088/1674-1056/ac3ba9

Generation of cavity-birefringence-dependent multi-wavelength bright-dark pulse pair in a figure-eight thulium-doped fiber laser

Xiao-Fa Wang(王小发), Dong-Xin Liu(刘东鑫), Hui-Hui Han(韩慧慧), Hong-Yang Mao(毛红炀)

Chin. Phys. B. 30, 054205 (2021). DOI: 10.1088/1674-1056/abd68f

Comparative study of pulsed laser diode end-pumped thulium-doped 2-μm Q-switched lasers

Ya Wen(温雅), Zhen Fan(范震), Lin-Hao Shang(尚林浩), Guang-Yong Jin(金光勇), Wang Chao(王超), Xin-Yu Chen(陈薪羽), Chun-Ting Wu(吴春婷)

Chin. Phys. B. 30, 034206 (2021). DOI: 10.1088/1674-1056/abca21

Generation and evolution of multiple operation states in passively mode-locked thulium-doped fiber laser by using a graphene-covered-microfiber

Xiao-Fa Wang(王小发), Jun-Hong Zhang(张俊红), Xiao-Ling Peng(彭晓玲), Xue-Feng Mao(毛雪峰)

Chin. Phys. B. 27, 084215 (2018). DOI: 10.1088/1674-1056/27/8/084215

Output characteristics of a 2.05 μm narrow-linewidth small-signal thulium-doped fiber amplifier under different pumping schemes

Xiaolong Sun(孙小龙)[1,2,3,4], Zhijian Huang(黄智健)[1,2,3,4], Miaomiao Yang(杨苗苗)[1,2,3,4], Menghua Jiang(姜梦华)[1,2,3,4,†], Tingwu Ge(葛廷武)[1,2,3,4], Wenbin Qin(秦文斌)[1,2,3,4], Youqiang Liu(刘友强)[1,2,3,4], Yinhua Cao(曹银花)[1,2,3,4], and Zhiyong Wang(王智勇)[1,2,3,4,‡]

[1] *School of Physics and Optoelectronic Engineering, Beijing University of Technology, Beijing* 100124, *China*
[2] *Beijing Engineering Research Center for Laser Application Technology, Beijing University of Technology, Beijing* 100124, *China*
[3] *Key Laboratory of Cross-Scale Laser Forming Manufacturing Technology, Ministry of Education, Beijing University of Technology, Beijing* 100124, *China*
[4] *Institute of Advanced Semiconductor Optoelectronic Technology, Laser Engineering Research Institute, Beijing University of Technology, Beijing* 100124, *China*

(Received 4 December 2025; revised manuscript received 13 January 2026; accepted manuscript online 11 February 2026)

This paper presents a study of the output characteristics of a 2.05 μm narrow-linewidth small-signal thulium-doped fiber amplifier under different pumping configurations. A 5 W seed source with a 2 kHz linewidth was modulated via an acousto-optic modulator and subsequently amplified in a fiber amplifier. Four pumping schemes were investigated: 1570 nm forward core pumping, 793 nm forward cladding pumping, simultaneous forward core-cladding pumping and forward core pumping combined with backward cladding pumping. Under conditions that suppress amplified spontaneous emission and stimulated Brillouin scattering, the corresponding output powers and slope efficiencies were 8.7 mW, 112 mW, 135 mW and 147 mW, and 0.4%, 5.5%, 5.6% and 6.1%, respectively. Among these, the scheme combining forward core pumping with backward cladding pumping demonstrated the best performance. The results demonstrate its potential as a high-power seed source for subsequent narrow-linewidth, high-energy fiber or solid-state amplification systems.

Keywords: thulium-doped fiber amplifier, small-signal, pumping configurations, amplified spontaneous emission (ASE), stimulated Brillouin scattering (SBS)

PACS: 42.55.Wd, 42.60.Da, 42.60.Lh, 42.65.Es

DOI: 10.1088/1674-1056/ae4461 **CSTR:** 32038.14.CPB.ae4461

1. Introduction

In recent years, 2 μm band laser technology has emerged as a research hotspot in the field of laser technology owing to its unique eye-safe characteristics,[1,2] atmospheric transmission window advantages[3] and coverage of water molecule absorption bands.[4] These properties make it highly valuable for applications such as environmental monitoring, lidar systems, biomedical diagnostics and nonlinear frequency conversion.[5–8] For instance, in differential absorption lidar systems, narrow-linewidth lasers enable precise discrimination between water vapor and carbon dioxide absorption lines in the atmosphere, achieving trace gas concentration inversion at sub-pm levels. In fiber-optic sensing, the narrow-linewidth feature significantly extends the coherence length of interferometers, enhancing the spatial resolution of distributed strain and temperature measurements. However, conventional 2 μm solid-state lasers face limitations such as bulky size, thermal management challenges and stability issues, hindering their suitability for high-precision, fully fiber-integrated applications. In contrast, fiber laser systems based on the master oscillator power amplifier architecture decouple the seed source from the power amplification stage, offering a promising pathway to simultaneously achieve narrow-linewidth operation and high-power output.

In the realm of 2 μm thulium-doped fiber (TDF) amplifiers, research efforts have been predominantly directed toward the design and optimization of high-power systems (hundreds of watts range).[9–12] In contrast, the specific scenario of narrow-linewidth, small-signal amplification has received comparatively less systematic investigation. This regime presents unique challenges, where the primary limitations shift from thermal management to the effective suppression of two critical nonlinear effects: amplified spontaneous emission (ASE) and stimulated Brillouin scattering (SBS).[13–21] ASE originates from the amplification of spontaneously emitted photons, and its intensity is closely linked to the length of the gain medium and pump power density. The SBS threshold is inversely proportional to the fiber's effective interaction length, optical intensity, and Brillouin gain coefficient. The choice of pumping strategy fundamentally influences the buildup of these effects. For narrow-linewidth, low-power signal amplification, three primary pumping schemes are employed: 793 nm cladding pumping, 1570 nm core pumping, and hybrid core-cladding pumping.[22–26] The 793 nm

†Corresponding author. E-mail: jmh@bjut.edu.cn
‡Corresponding author. E-mail: zywang@bjut.edu.cn

© 2026 Chinese Physical Society and IOP Publishing Ltd. All rights, including for text and data mining, AI training, and similar technologies, are reserved.

cladding pumping method, which utilizes the $^3H_6 \rightarrow {}^3F_4$ transition of Tm^{3+} ions and benefits from the cross-relaxation process (theoretical quantum efficiency up to 200%), enables high-power operation. However, in a forward cladding-pumped TDF at 793 nm, the highest gain at the pump end strongly amplifies backward-propagating ASE. This depletes the front-section population inversion, impairing signal amplification there and forcing greater reliance on the middle and rear fiber gain. Consequently, overall gain efficiency drops while conditions favoring forward ASE generation are enhanced, leading to significant ASE in the output. Concurrently, the high signal power density achievable with this approach significantly lowers the threshold for SBS. The 1570 nm core pumping scheme directly excites Tm^{3+} ions to the $^3F_4$ energy level, offering lower quantum defects and excellent compatibility with single-mode pumping, and its inherently lower and more distributed gain profile is advantageous for suppressing ASE accumulation. However, its application remains limited due to weak absorption of Tm^{3+} at 1570 nm (absorption coefficient < 1 dB/m), resulting in low pump light utilization efficiency and poor slope efficiency, which in turn keeps signal power levels well below the SBS threshold. The hybrid core-cladding pumping approach synergistically combines 793 nm and 1570 nm dual-wavelength pumping, effectively enhancing energy extraction efficiency and boosting output power. This strategy addresses the limitations of individual pumping methods while leveraging their complementary advantages, making it a promising candidate for high-performance narrow-linewidth amplification systems.

This study focuses on optimizing pumping strategies for a 2.05 μm narrow-linewidth low-signal TDF amplifier. A 5 W seed source with a 2 kHz linewidth was first pulse-modulated via an acousto-optic modulator (AOM) and subsequently amplified in a TDF amplifier. Four pumping schemes were systematically investigated: 1570 nm forward core pumping, 793 nm forward cladding pumping, simultaneous forward core-cladding pumping, and core-forward and cladding-backward pumping. Under conditions of suppressed ASE and SBS, the output powers of the four schemes were determined, with the core-forward and cladding-backward pumping configuration achieving the highest performance with an output power of 147 mW. This optimized scheme demonstrates its potential as a high-quality seed source for subsequent amplification in 2 μm narrow-linewidth high-energy laser systems.

2. Experimental setup

The experimental configuration is illustrated in Fig. 1. A 2.05 μm narrow-linewidth fiber seed source with an output power of 5 W and a linewidth of 2 kHz was first isolated and then pulse-modulated using an AOM. The modulation generated Gaussian-like pulses with a width of 800 ns and a repetition rate of 4 kHz. Due to the narrow linewidth of the seed source, the SBS threshold during amplification was relatively low. To monitor backward-propagating light during amplification, a circulator was connected after the AOM. The amplification stage employed a 2 m long double-clad TDF with a core/cladding diameter of 10/130 μm from NuFern, and its doping concentration was approximately 5×10^{25} m^{-3}, with an absorption coefficient of 9.6 dB/m at 793 nm. As a critical design parameter, the fiber length requires a careful trade-off between pump absorption, gain distribution and suppression of nonlinear effects. The 2 m length of TDF adopted in this work was primarily determined by the following considerations. First, the absorption coefficient of the fiber at 793 nm is approximately 9.6 dB/m. A 2 m length ensures that the majority of the pump light is absorbed, avoiding either pump waste due to a shorter fiber or excessive front-section gain caused by a longer fiber, which would intensify backward ASE. Second, for the optimal hybrid "forward-core/backward-cladding" pumping scheme, this length allows the preliminary gain produced by the 1570 nm forward pump and the main gain region provided by the 793 nm backward pump to be clearly separated and efficiently coupled; after receiving moderate amplification in the front section, the signal enters the high-gain rear section with already appreciable power, enabling efficient gain extraction and thereby suppressing ASE. Furthermore, selecting a 2 m length is an active measure to control the effective interaction length and raise the SBS threshold. Figure 1(a) shows forward core pumping using a 1570 nm fiber pump source (2 W output power) coupled into the TDF via a wavelength-division multiplexer (WDM), and the WDM exhibits approximately 80% transmission at 2.05 μm and about 85% reflection at 1570 nm. Figure 1(b) shows forward cladding pumping using a 793 nm semiconductor pump source (8 W output power) injected through a $(2+1) \times 1$ pump combiner with the residual pump light being stripped using a cladding power stripper (CPS) after the TDF. Figure 1(c) shows simultaneous forward core-cladding pumping using both 1570 nm and 793 nm pump sources. Figure 1(d) illustrates core-forward and cladding-backward pumping. The isolator and circulator introduced approximately 20% loss to the seed laser, while the pump combiner exhibited negligible loss. Taking into account the insertion losses of the aforementioned components, the signal power entering the TDF from the modulated seed was 3.3 mW for the forward cladding pumping scheme shown in Fig. 1(b) and 2.6 mW for the other three pumping configurations. Note that for clarity of presentation, the front-end structures of several experimental configurations have been merged in Fig. 1. In the actual experiments, each configuration was tested independently, and the optical path was not split after the circulator. Moreover, the experimental setup did not adopt either the backward core pumping scheme or the cladding-forward and backward core pumping scheme, mainly for the following two reasons. First,

implementing backward core pumping would require the insertion of an additional filter between the TDF and the circulator to remove the residual 1570 nm pump laser, thereby introducing extra insertion loss. Furthermore, the WDM itself would also attenuate the amplified signal light by approximately 20%. Second, backward core pumping would fail to provide initial gain in the front section of the fiber where the signal is weak, likely resulting in a more uneven gain distribution along the entire fiber and impairing efficient extraction of the small-signal input. Similarly, a hybrid scheme combining forward cladding pumping and backward core pumping would likely resemble the already tested "forward core combined with backward cladding" configuration, but the contribution of the 1570 nm pump would be even weaker because its injection from the rear end offers no assistance to the initial signal amplification. Additionally, since the 1570 nm backward pump propagates opposite to the signal, the region of high population inversion would be closer to the signal output end, making it easier for ASE to be amplified and emitted.

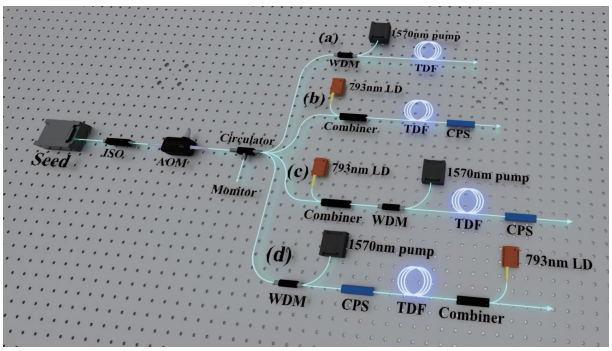


Fig. 1. Diagram of the experimental setup: (a) forward core pumping; (b) forward cladding pumping; (c) simultaneous forward core-cladding pumping; (d) core-forward and cladding-backward pumping.

3. Result and discussion

3.1. Forward core pumping

The experimental results for forward core pumping using a 1570 nm pump source are shown in Fig. 2. Figure 2(a) shows the amplified signal power curve, revealing an output power of 8.7 mW at a pump power of 2 W, corresponding to a slope efficiency of 0.4%. Due to losses from the isolator, circulator, and WDM, the signal power entering the TDF after AOM modulation was reduced to about 2.6 mW. The low small-signal gain of the TDF, combined with its inherent absorption at the signal wavelength, resulted in extremely poor amplification efficiency. Figure 2(b) illustrates the output spectrum at 8.7 mW; it exhibits two distinct peaks at 1570 nm (residual pump laser) and 2051 nm (amplified signal), along with weak ASE in the 1900–2000 nm range. To quantify the contributions of the residual pump laser and ASE, the spectrum was converted to a linear scale, and the integrated power of the three peaks was analyzed. The residual pump light accounted for only about 0.9%, while ASE contributed about 1.9%, both negligible relative to the signal. Additionally, the backward-propagating power monitored via the circulator was 38 μW, indicating no significant SBS during the amplification. While forward core pumping at 1570 nm achieved ASE and SBS suppression, its low amplification efficiency and limited output power restricted its applicability in high-power scenarios. Increasing the pump power could marginally improve output power, but the inherent inefficiency and ASE accumulation ultimately constrain the scalability. These results underscore the limitations of core-pumping strategies for narrow-linewidth low-signal amplification in 2.05 μm systems.

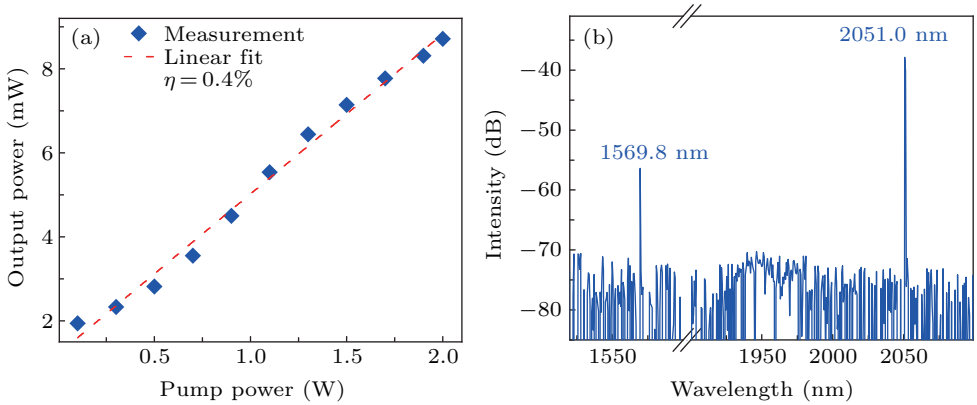


Fig. 2. Experimental results for forward core pumping: (a) amplified power curve; (b) forward output spectrum.

3.2. Forward cladding pumping

The experimental results for forward cladding pumping using a 793 nm semiconductor pump source are presented in Fig. 3. Figure 3(a) shows the output power curve with an amplified signal power of 141 mW at a pump power of 3.8 W, corresponding to a slope efficiency of 5.5%, which is significantly higher than that of forward core pumping. This improvement can be attributed to the higher available pump power at 793 nm and the stronger absorption coefficient of the TDF at 793 nm compared with 1570 nm. At 3.8 W pump power, the output spectrum exhibited prominent ASE, as shown in Fig. 3(b). Conversion to a linear scale revealed that ASE contributed about 40% to the total output. When the pump power was

reduced to 3.4 W, the output power decreased to 112 mW and ASE was negligible (about 4% contribution), as shown in Fig. 3(c). Figure 3(d) shows the backward-propagating spectrum monitored via the circulator at 3.4 W pump power; it displays a weak Stokes peak at 2051.1 nm (adjacent to the main signal peak at 2051.0 nm), indicating the onset of SBS. However, its intensity (38 μW) remains too low to significantly impact amplifier performance. Despite ASE limitations at higher pump powers, forward cladding pumping with a 793 nm source achieved a substantial increase in output power (141 mW versus 8.7 mW for forward core pumping) while maintaining manageable SBS levels. This validates its effectiveness as a viable strategy for narrow-linewidth low-signal amplification at 2.05 μm.

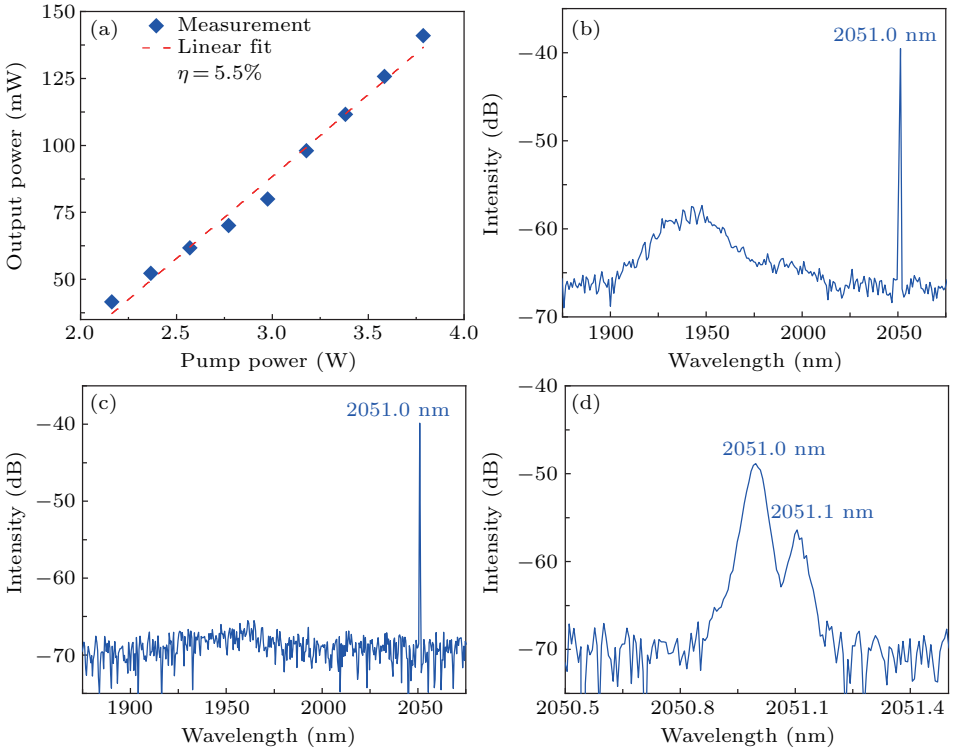


Fig. 3. The experimental results for forward cladding pumping: (a) amplified power curve; (b) and (c) forward output spectra when the pump power is 3.8 W or 3.4 W, respectively; (d) backward output spectrum at a pump power of 3.4 W.

3.3. Simultaneous forward core-cladding pumping

To further explore the optimal pumping strategy for 2.05 μm narrow-linewidth low-signal amplification, simultaneous forward core-cladding pumping was implemented using both 1570 nm and 793 nm pump sources. The results are summarized in Fig. 4. Figure 4(a) is the amplification power curve obtained by first increasing the 1570 nm pump power to 2 W and then incrementally adding 793 nm pump power. The 1570 nm pump exhibits persistently low efficiency, while the 793 nm pump achieves a slope efficiency similar to that of standalone cladding pumping. At a total pump power of 5.2 W, the output power reaches 158 mW. Figure 4(b) shows the forward output spectrum at 5.2 W pump power, revealing strong ASE, with ASE contributing about 32% of the total power. Reducing the 793 nm pump power to achieve a total pump power of 4.9 W lowered the ASE contribution to about 8%, as shown in Fig. 4(c), yielding an output power of 135 mW. Figure 4(d) illustrates the backward-propagating spectrum at 4.9 W pump power, displaying a weak Stokes peak at 2051.1 nm (adjacent to the main signal peak at 2051.0 nm), confirming the presence of low-level SBS with negligible impact. The simultaneous forward core-cladding pumping scheme amplifies the signal from 2.6 mW to 135 mW, achieving a 20% power increase compared with standalone forward cladding pumping. This hybrid approach demonstrates enhanced efficiency while maintaining acceptable ASE and SBS levels, making it a superior pumping strategy for narrow-linewidth low-signal amplification in 2.05 μm systems.

3.4. Core-forward and cladding-backward pumping

The final pumping strategy tested combined 1570 nm core-forward pumping and 793 nm cladding-backward pumping; the results are shown in Fig. 5. Similar to the simultaneous forward core-cladding pumping scheme, the 1570 nm pump power was first increased to 2 W, followed by incremental addition of 793 nm pump power. Figure 5(a) shows the amplification power curve with an output power of 163 mW at a total pump power of 5.1 W. Figure 5(b) illustrates that the forward output spectrum exhibits no detectable ASE, indicating superior ASE suppression. It can be observed that compared with forward cladding pumping, the forward core pumping

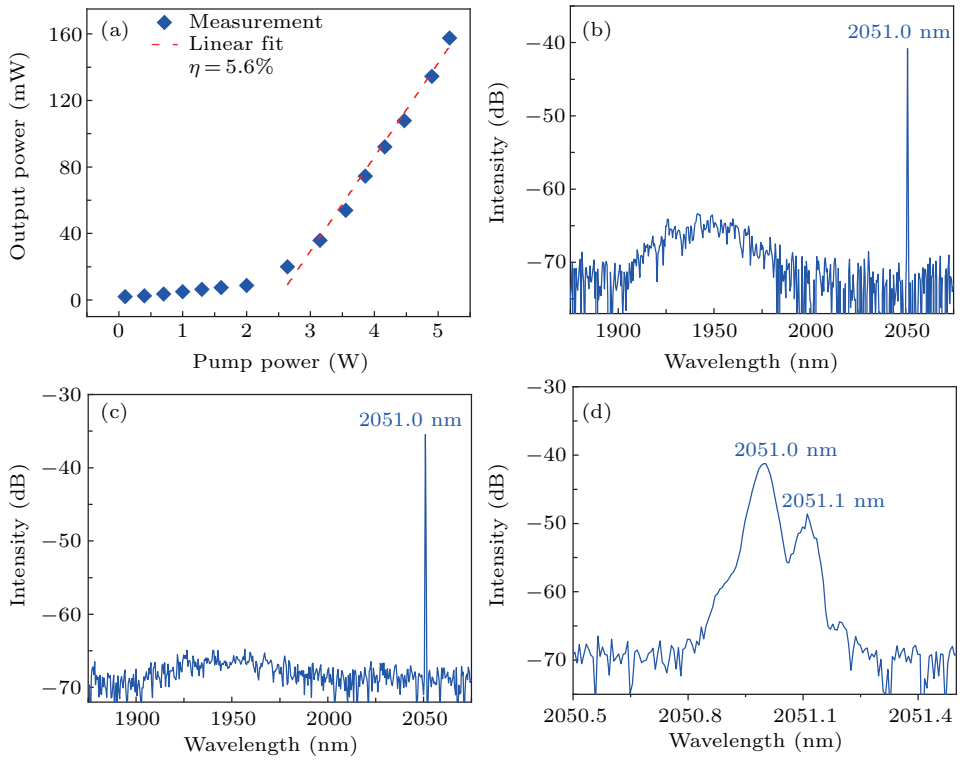


Fig. 4. The experimental results for simultaneous forward core-cladding pumping: (a) amplified power curve; (b) and (c) forward output spectra when the pump power is 5.2 W or 4.9 W, respectively; (d) backward output spectrum at a pump power of 4.9 W.

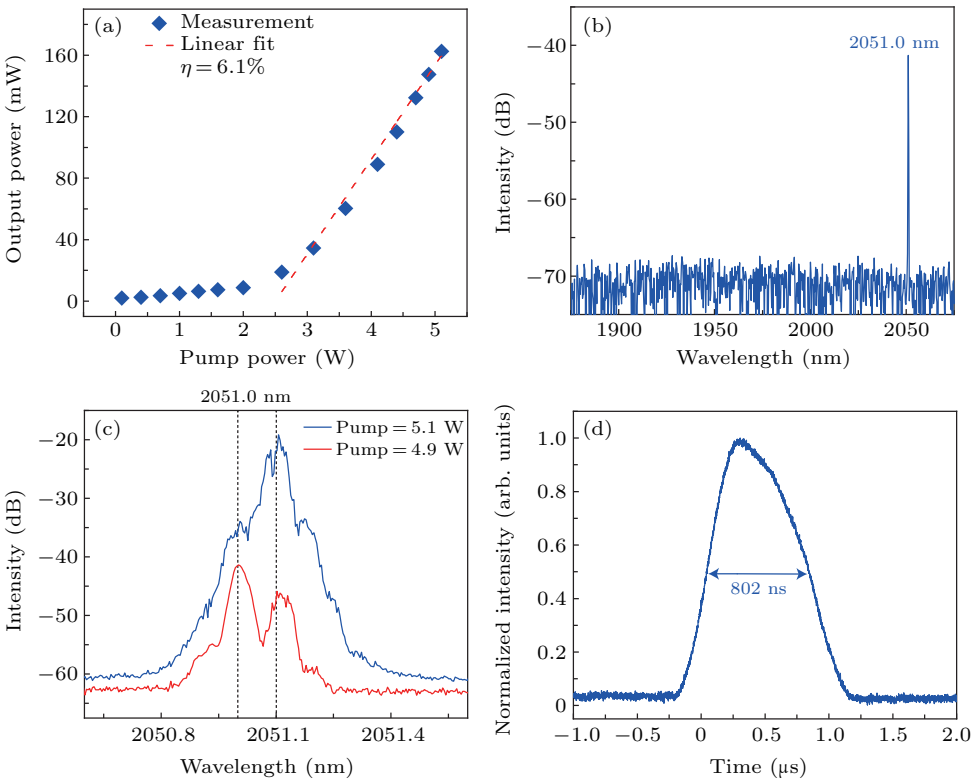


Fig. 5. The experimental results for simultaneous core-forward and cladding-backward pumping: (a) amplified power curve; (b) forward output spectrum; (c) backward output spectra at pump powers of 5.1 W and 4.9 W; (d) pulse width.

combined with 793 nm backward cladding pumping scheme demonstrates superior ASE suppression. The underlying reasons are analyzed as follows. In the case of 793 nm backward pumping, the pump power is strongest at the fiber output end and decreases toward the input end. Although the forward-propagating ASE passes through the high-gain rear section, the signal laser in this region has already reached a substantial intensity and consumes the available population inversion, suppressing the gain accessible to ASE. Furthermore, the forward core pumping provides a moderate and relatively uni-

form initial gain in the front section of the fiber, which elevates the signal power to a certain level before it enters the high-gain region dominated by the 793 nm backward pump. This optimized gain distribution along the fiber effectively inhibits the generation and buildup of ASE. As shown in Fig. 5(c), curves A and B display the backward-propagating spectrum at pump powers of 5.1 W and 4.9 W, respectively. Spectrum A reveals a strong Stokes signal generated by SBS that exceeds the intensity of the 2051 nm reflected signal. This SBS can be attributed to the increased effective fiber length caused by the pigtail of the backward pump combiner, which lowers the SBS threshold according to the general SBS threshold formula

$$P = \frac{GA_{\text{eff}}}{g_0 L_{\text{eff}}}, \tag{1}$$

where P is the SBS threshold, G is the threshold gain coefficient, A_{eff} is the effective mode area, g_0 is the Brillouin gain coefficient and L_{eff} is the effective fiber length. Hence shortening the pump combiner pigtail reduces the effective fiber length, suppressing SBS. At 4.9 W total pump power (spectrum B), the output power stabilizes at 147 mW, with the backward spectrum showing a Stokes signal weaker than the 2051 nm reflection peak. Figure 5(d) shows the pulse width of the amplified laser measured with an oscilloscope, which is approximately 802 ns and in good agreement with the pulse width set by the AOM. The hybrid core-forward/cladding-backward pumping scheme achieved an output power of 147 mW, representing improvements of 31% and 9% over standalone cladding-forward pumping and simultaneous forward core-cladding pumping, respectively. This configuration effectively suppresses ASE while balancing SBS limitations, making it the most power-efficient pumping strategy for 2.05 μm narrow-linewidth low-signal amplification. On the other hand, despite its performance advantages, the higher cost of 1570 nm pump sources and the complexity of hybrid pumping architectures must be weighed against the simplicity and cost-effectiveness of 793 nm cladding pumping. System designers should prioritize application-specific requirements such as power, noise tolerance, budget and so on when selecting a pumping scheme.

4. Conclusion

This study comprehensively investigated the output characteristics of a 2.05 μm narrow-linewidth low-signal fiber amplifier under four distinct pumping schemes, analyzing ASE contributions and monitoring SBS through backward-propagating spectral measurements. Experimental results demonstrated that the core-forward and cladding-backward pumping configuration outperformed others, achieving a 31% and 9% power improvement over standalone cladding-forward and simultaneous core-cladding pumping, respectively. These findings establish a robust framework for advancing high-quality seed sources in narrow-linewidth high-energy 2 μm laser systems, offering critical insights for power scaling.

Acknowledgment

Project supported by the Beijing Natural Science Foundation (Grant No. L241061).

References

[1] Zhang J, Liu P, Xu X, Xu X D, Yan D Y, Li D Z and Xu J 2017 *Opt. Mater.* **73** 675
[2] Miluski P, Michalska M, Kochanowicz M, Markowski K, Łodziński M and Pisarski W A 2024 *J. Lightwave Technol.* **42** 3844
[3] Yang Y, Shutler A and Grischkowsky D 2011 *Opt. Express* **19** 8830
[4] Iwai H and Aoki M 2023 *Opt. Express* **31** 13817
[5] Liu Z L, Barlow J F, Chan P W, Fung J C H, Li Y G, Ren C, Mark H W L and Ng E 2019 *Remote Sens.* **11** 2522
[6] Molebny V, McManamon P F, Steinvall O, Kobayashi T and Chen W B 2016 *Opt. Eng.* **56** 031220
[7] Bai Z X, Zhao Z G, Tian M H, Jin D, Pang Y J, Li S S, Yan X S, Wang Y L and Lu Z W 2022 *Microwave Opt. Technol. Lett.* **64** 2244
[8] Gu R Y, Li Z L, Lei C, Li S, Wang D and Wang X H 2023 *J. Med. Biol. Eng.* **43** 351
[9] Liu J, Shi H X, Liu K, Hou Y B and Wang P 2014 *Opt. Express* **22** 13572
[10] Guan X C, Yang C S, Gu Q, Lin W, Tan T Y, Zhao Q L, Wei X M, Yang Z G and Xu S H 2021 *Appl. Phys. Express* **14** 112004
[11] Wang X, Jin X X, Wu W J, Zhou P, Wang X L and Xiao H 2015 *IEEE Photon. Technol. Lett.* **27** 677
[12] Wang X, Jin X X, Zhou P, Wang X L, Xiao H and Liu Z J 2015 *IEEE Photon. Technol. Lett.* **27** 1473
[13] Ren C Y, Han Y C, Luan X Y, Jiang H, Wang F, Wang H T and Shen D Y 2025 *Opt. Lett.* **50** 1200
[14] Yu M, Jin G Y, Wang J and Wu C T 2020 *Infrared Phys. Techn.* **105** 103173
[15] Ren J J, Qi Y F, Yu T, Tao M M, He Z X and Ye X S 2024 *Opt. Express* **32** 31566
[16] Sincore A, Bodnar N, Bradford J, Abdulfattah A, Shah L and Richardson M C 2017 *J. Lightwave Technol.* **35** 4000
[17] Tsvetkov S V, Khudyakov M M, Lobanov A S, Lipatov D S, Bubnov M M and Guryanov A N 2021 *J. Lightwave Technol.* **39** 592
[18] Ren J J, Qi Y F, He Z X, Yu T and Ye X S 2025 *Opt. Fiber Technol.* **90** 104103
[19] Cheng R J, Li X X, Wang Q, Liu D J, Huang Z M, Lv S Y, Zhou Y Z, Zhang S T, Li X M, Chen Z J, Wang Q, Liu Z J, Cao L H and Zheng C Y 2024 *Chin. Phys. B* **33** 015206
[20] Yang Q, Li Y, Zou H, Mei Q, Xu E M and Zhang Z X 2024 *Chin. Phys. B* **33** 024206
[21] Xu G X, Kang N, Lei A L, Liu H Y, Zhao Y, Zhou S L, An H H, Xiong J, Wang R R, Xie Z Y, Zhou X C, Fang Z H and Wang W 2024 *Chin. Phys. B* **33** 085204
[22] Yin T C, Song Y F, Jiang X G, Chen F H and He S L 2019 *Opt. Express* **27** 15794
[23] Qiao T, Cheng H H, Wen X X, Wang W L, Lin W, Zhou Y, Guo Y K, Liu Y C and Yang Z M 2019 *Opt. Lett.* **44** 6001
[24] Khamis M A and Ennser K 2016 *J. Lightwave Technol.* **34** 5675
[25] Tench R. E, Romano C and Delavaux J M 2018 *Opt. Fiber Technol.* **42** 18
[26] Romano C, Tench R E and Delavaux J M 2018 *Opt. Express* **26** 26080